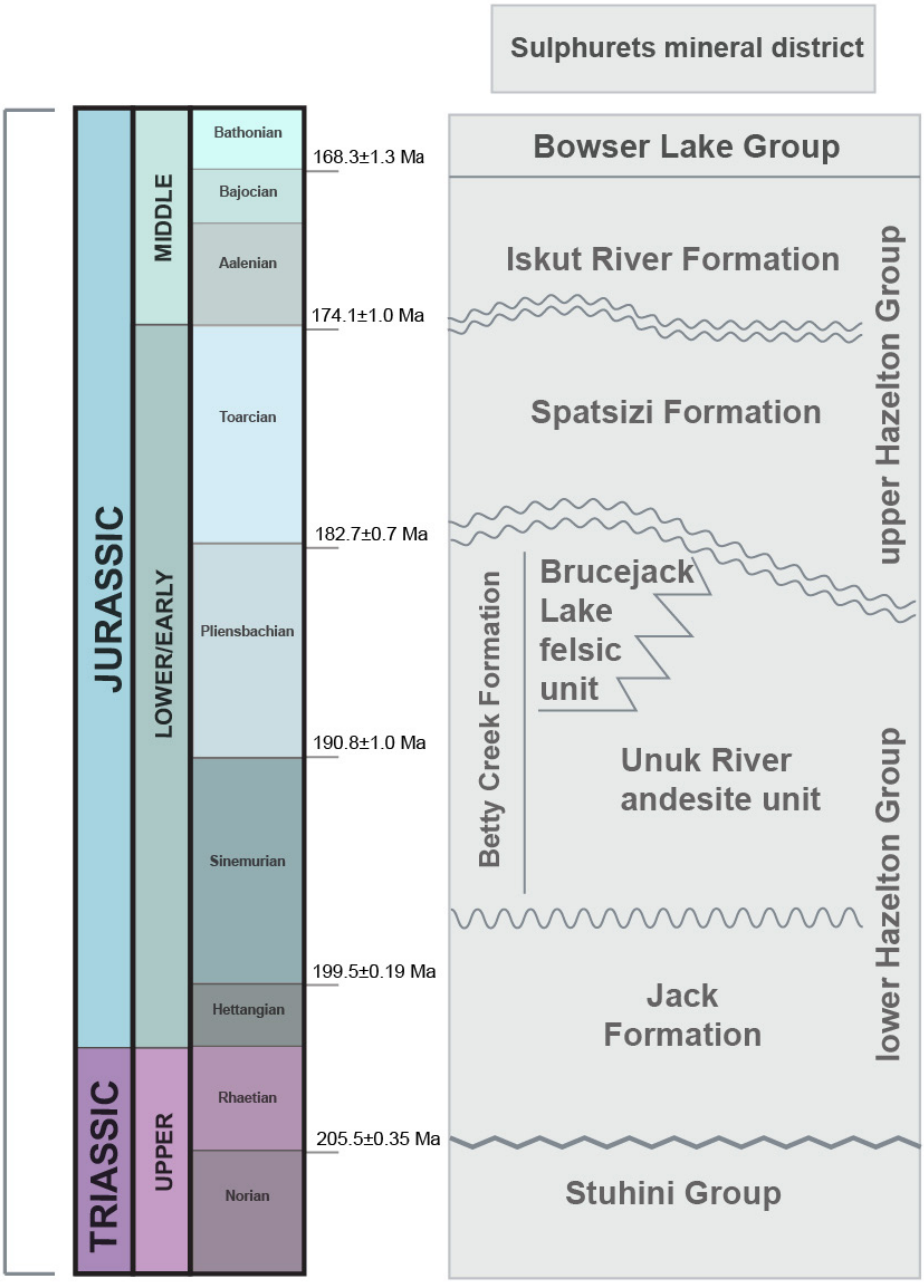

Fig. A1. Hazelton Group stratigraphic nomenclature in the Sulphurets mineral district. Modified after Nelson et al. (2018).

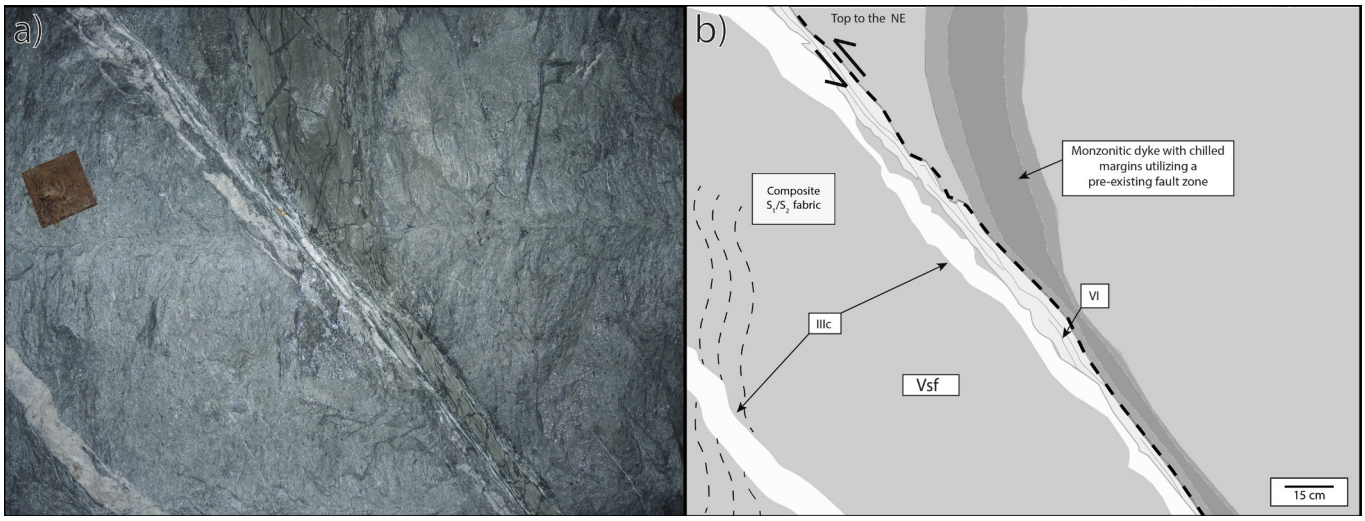

Fig. A2. Underground exposure (a) and schematic interpretation (b) of an intermediate to mafic dike (ca.183 Ma) with visible chilled margins, utilizing a pre-existing fault that was, in turn, previously utilized by a mineralized Stage IIIc quartz-calcite vein (IIIc). Both the early vein and dike cut the composite foliation. Re-activation of the same structure during post-mineralization thrusting accompanied by quartz-Stage VI chlorite shear vein (VI) development. Valley of the Kings zone.

Fig. A3. Photo of an underground exposure showing a buckled and partly dismembered Stage II quartz veinlet (II) in a silicified zone at the base of the Conglomerate unit in the Valley of the Kings zone (after Sillitoe, 2015). A stage III quartz-carbonate veinlet (~2 cm wide; III) cuts the silicified zone and the Stage II veinlet. Py = pyrite.

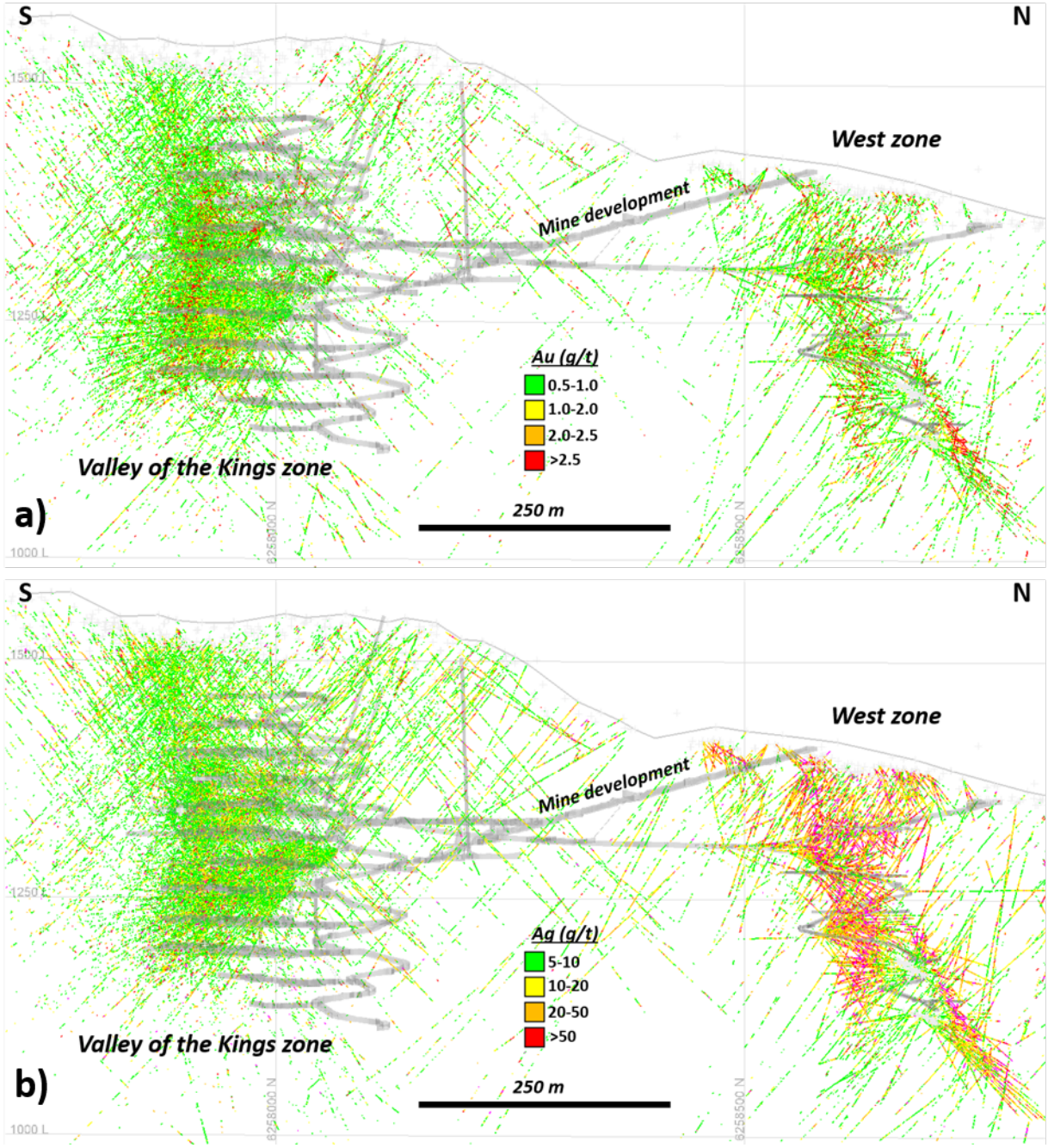

Fig. A4. South to north cross sections showing gold and silver distribution in the Brucejack deposit. Current mine workings are shown for reference. a) Gold mineralization appears, on the deposit scale, to be more structurally continuous (channelized flow) in the West zone and more disseminated (pervasive flow) in the Valley of the Kings zone. Bonanza grade intersections are locally present throughout the deposit, but do not define obvious mineralized trends in the Valley of the Kings zone. The significant low-grade halo associated with pyrite-hosted gold is readily apparent. b) Silver mineralization is zoned across the deposit, with the West zone being significantly more silver-rich than the Valley of the Kings zone. Abundant silver sulfosalt minerals (see Table 2) are present, in addition to electrum, in the West zone. Silver mineralization in the Valley of the Kings zone is largely limited to electrum. The reason behind the silver enrichment in the West zone is under investigation, particularly its significance as an exploration vector.

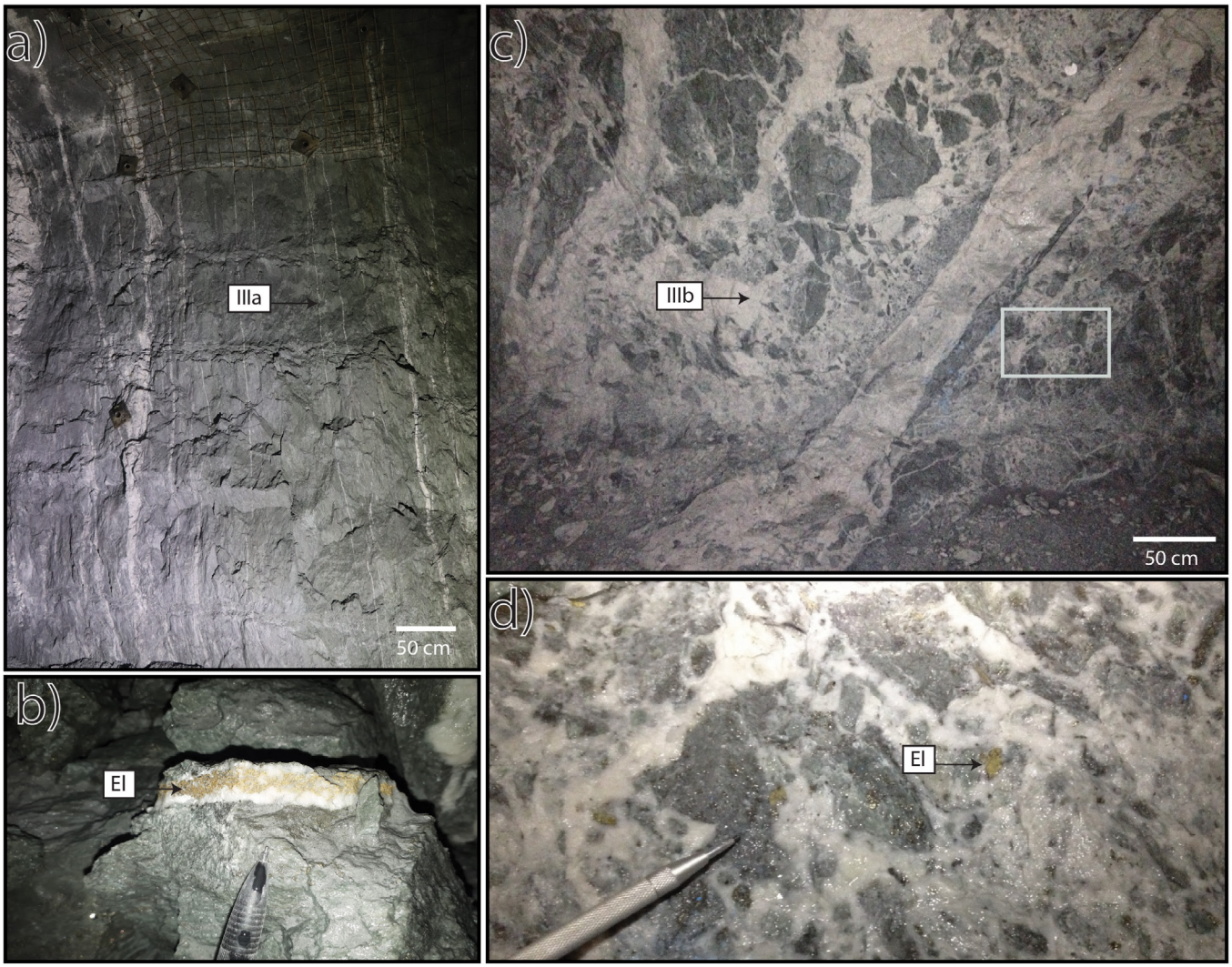

Fig. A5. Photos illustrating erratic electrum distribution in the Valley of the Kings zone. a) and b) Subvertical sheeted Stage IIIa veins (IIIa) in underground exposure and visible dendritic electrum-rich Stage III in muck from the same round: overall sheeted Stage III vein corridors contain abundant electrum (El), however electrum occurrences are seemingly locally randomly distributed within individual veins. c) and d) Visible clots of dendritic electrum hosted in multistage Stage IIIb quartz-carbonate stockwork breccia (IIIb): dendritic clots of electrum occur in apparently random clusters in different parts of the breccia matrix and in contact with host rock breccia fragments.

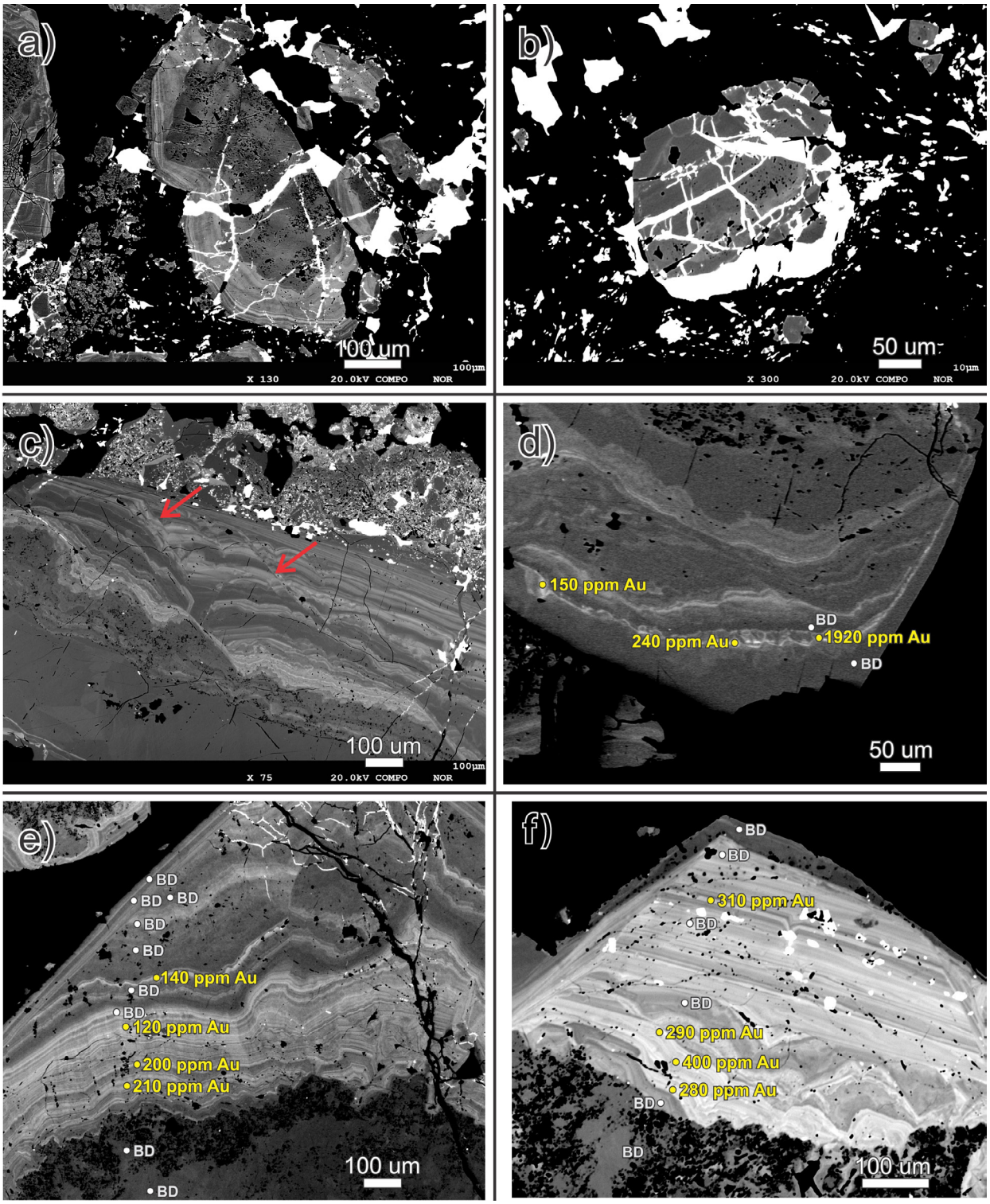

Fig. A6. Backscattered-electron (BSE) images of pyrite and electrum from ore-stage quartz-carbonate veins and phyllically altered wall rock at the Brucejack deposit. a) and b) Electrum (brightest mineral) cuts oscillatory zoned arsenian pyrite (As-rich bands of pyrite are lighter colored and surround an As-poor pyrite core). c) Pre-electrum deformation of the arsenian pyrite is manifested by several groups of microfractures (red arrows) in the pyrite, which offset intermediate arsenian pyrite bands but do not propagate into the outermost pyrite growth zones. d), e), and f) Electron microprobe wavelength dispersive spectrometer (EMPA-WDS) spot analyses of pyrite indicate significant Au concentrations in irregularly shaped, intermediate, arsenian growth zones (yellow dots), whereas As-poor cores and outer growth zones all have Au concentrations below detection limit (gray dots labeled "BD"; i.e., <100 ppm Au).

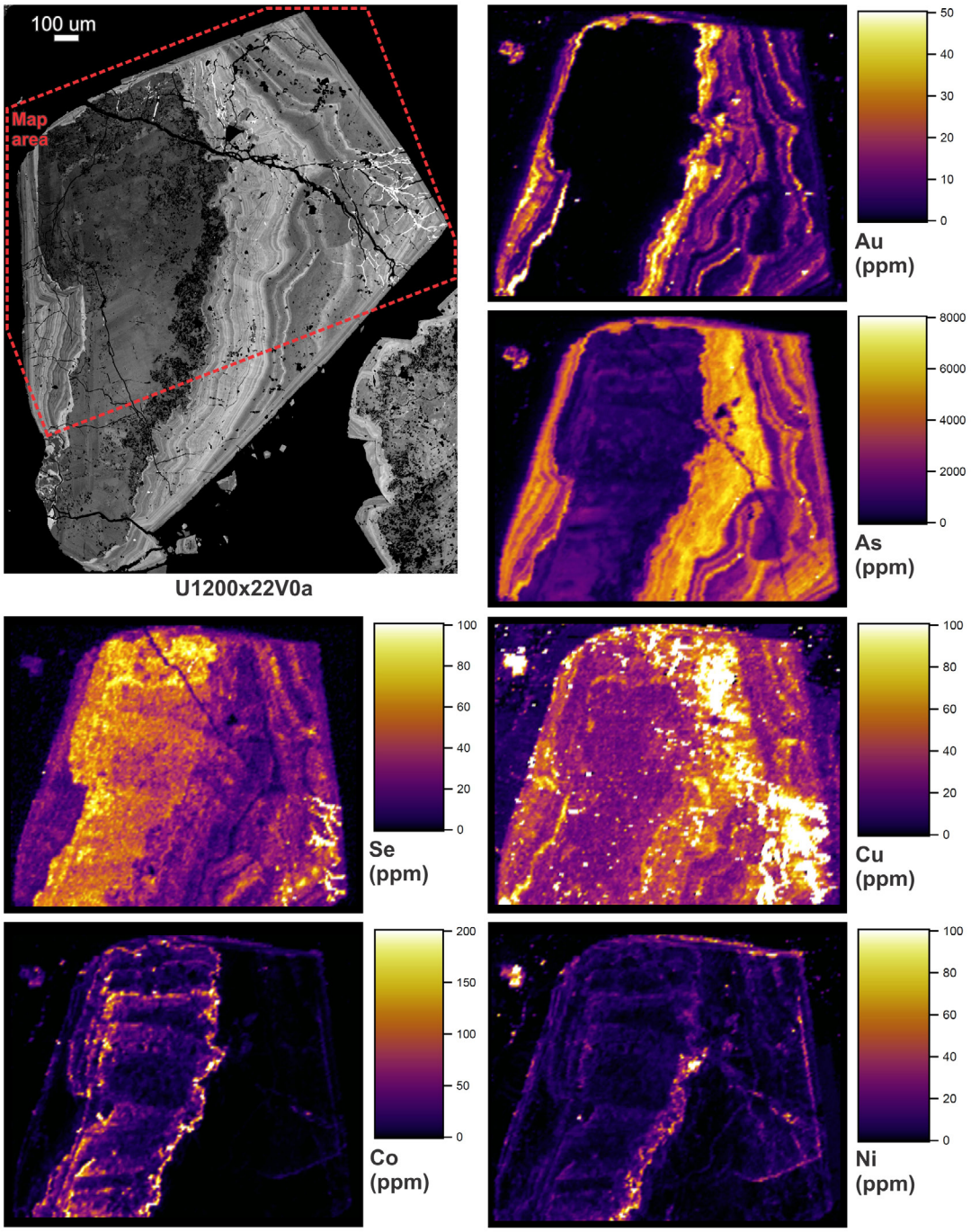

Fig. A7. Laser ablation inductively coupled plasma mass spectrometry (LA-ICP-MS) elemental maps of a pyrite grain sampled from an early discontinuous pyrite-stringer vein (Stage I) in the Valley of the Kings underground mine workings, shown in reference to the grain before ablation (BSE image, top left). The core of the pyrite locally displays cubic growth zonation defined by the periodic occurrence of angular to subangular bands enriched in Co, Ni, and Se. Corrosion and dissolution of the pyrite core is evidenced by the highly irregular shape of its rims and the presence of cavities along and proximal to the rims. Overgrowing the pyrite core is a large intermediate area of oscillatory-zoned pyrite which is characterized by delicate (<10 μm wide), wispy to colloform bands that are strongly enriched in As, Au, Cu, and weakly enriched in Ag and Mo (Ag and Mo maps not shown; chalcopyrite and Cu-Ag sulfosalt mineralization filling fractures in the central and right portions of the grain are responsible for the >100 ppm anomalies in the Cu map). These bands are locally truncated by grain boundaries. Collectively, these textures are interpreted to evidence transitional porphyry to epithermal conditions prior to electrum formation in the Valley of the Kings zone and are strikingly similar to those described for the "composite" pyrite grain type at the Lihir epithermal-porphyry deposit (i.e., porphyry-stage pyrite grains that were modified during subsequent epithermal-stage hydrothermal activity; Sykora et al., 2018).

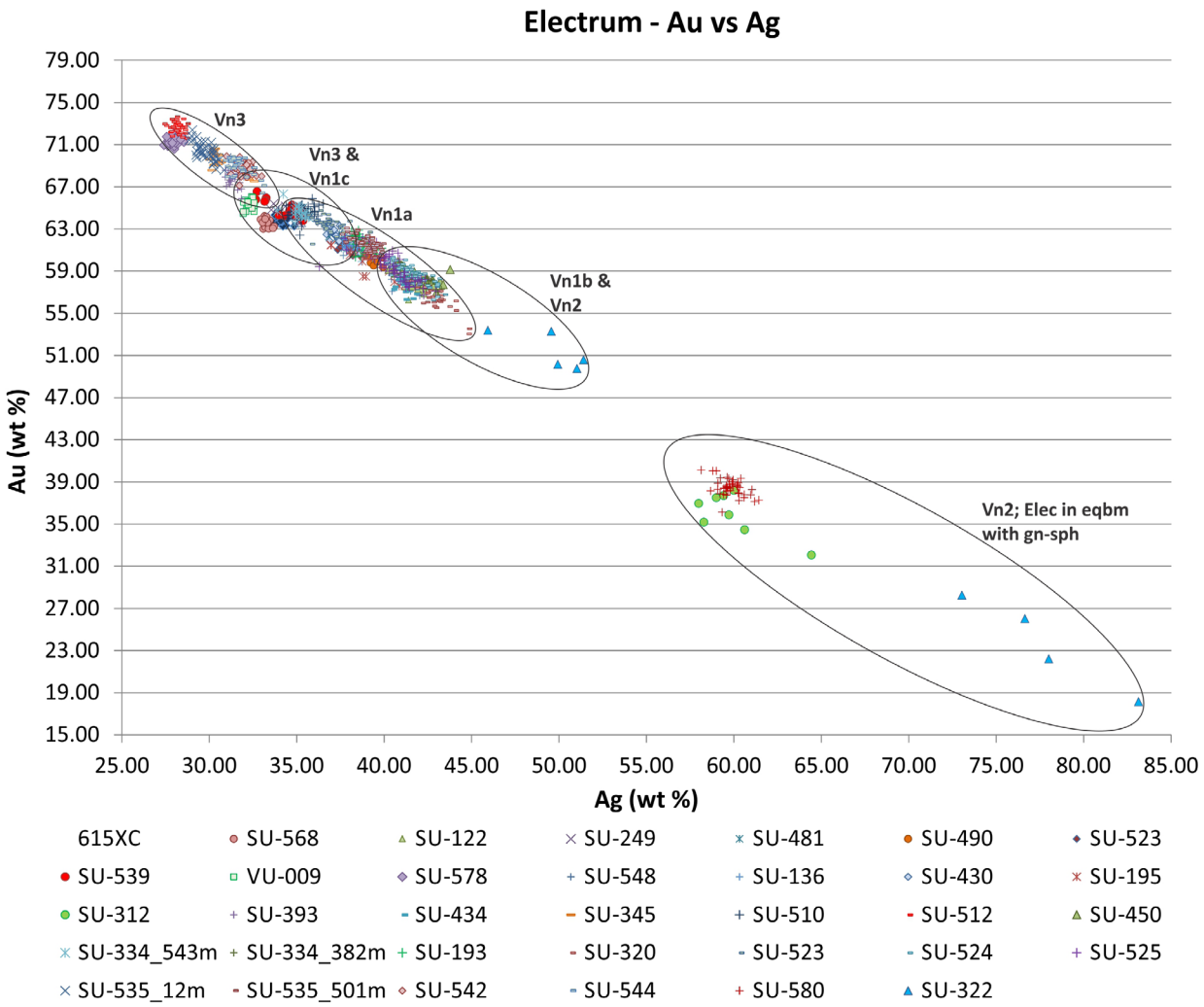

Fig. A8. Gold and silver concentrations in electrum from the Valley of the Kings zone based on EMPA-WDS analyses: the Au:Ag ratio of the electrum appears to vary considerably with vein type; no significant variation in the Au:Ag ratio of electrum is observed within individual samples except where electrum is locally in textural equilibrium with galena and sphalerite within the Vn2 vein generation.